

Morphometry of corpus callosum in Williams syndrome: shape as an index of neural development

Adriana Sampaio · Sylvain Bouix · Nuno Sousa ·
Cristiana Vasconcelos · Montse Fernández ·
Martha E. Shenton · Óscar F. Gonçalves

Received: 15 December 2011 / Accepted: 25 April 2012 / Published online: 22 May 2012
© Springer-Verlag 2012

Abstract Brain abnormalities in Williams syndrome (WS) have been consistently reported, despite few studies have devoted attention to connectivity between different brain regions in WS. In this study, we evaluated corpus callosum (CC) morphometry: bending angle, length, thickness and curvature of CC using a new shape analysis method in a group of 17 individuals with WS matched with a typically developing group. We used this multimethod approach because we hypothesized that neurodevelopmental

abnormalities might result in both volume changes and structure deformation. Overall, we found reduced absolute CC cross-sectional area and volume in WS (mean CC and subsections). In parallel, we observed group differences regarding CC shape and thickness. Specifically, CC of WS is morphologically different, characterized by a larger bending angle and being more curved in the posterior part. Moreover, although CC in WS is shorter, a larger relative thickness of CC was found in all callosal sections. Finally, groups differed regarding the association between CC measures, age, white matter volume and cognitive performance. In conclusions, abnormal patterns of CC morphology and shape may be implicated in WS cognitive and behavioural phenotype.

A. Sampaio and S. Bouix share equal first authorship.

A. Sampaio (✉) · Ó. F. Gonçalves
Neuropsychophysiology Laboratory, CiPsi, School
of Psychology, University of Minho, Braga, Portugal
e-mail: adriana.sampaio@psi.uminho.pt

S. Bouix (✉) · M. E. Shenton
Psychiatry Neuroimaging Laboratory, Department of Psychiatry,
Brigham and Women's Hospital, Harvard Medical School,
1249 Boylston Street, Boston, MA 02215, USA
e-mail: sylvain@bwh.harvard.edu

N. Sousa
Life and Health Sciences Research Institute,
University of Minho, Braga, Portugal

C. Vasconcelos
Department of Neuroradiology, Hospital de Santo António,
Porto, Portugal

M. Fernández
Genetic Molecular Unit, Galician Public Foundation of Genomic
Medicine, University of Santiago de Compostela,
Santiago de Compostela, Spain

M. E. Shenton
Laboratory of Neuroscience, Clinical Neuroscience Division,
Department of Psychiatry, VA Boston Healthcare System,
and Harvard Medical School, Brockton, MA, USA

Keywords Corpus callosum · MRI · Neurodevelopment · Williams syndrome

Introduction

Williams syndrome (WS) is a rare genetically determined neurodevelopmental disorder with an estimated prevalence of 1 in 7,500 live births (Strømme et al. 2002) and is caused by a hemideletion on chromosome 7q11.23 (Ewart et al. 1993). Associated with this genotype, WS patients display an unusual cognitive phenotype, characterized by intellectual disabilities with a distinctive neuropsychological profile, with peaks and valleys of abilities. Specifically, severe impairments in visuo-spatial cognition coexist with a relative preservation of face recognition, language and narrative skills (Bellugi et al. 2000). One of the most striking features of individuals with WS is their distinct social-affective profile, characterized by high sociability, disinhibition, over-friendliness (Bellugi et al. 1999; Klein-Tasman and

Mervis 2003) and strong empathy (Klein-Tasman and Mervis 2003).

This cognitive/behavioural phenotype has also been associated with several neuroanatomic changes, including volumetric and morphological changes, as well as abnormal asymmetry patterns (Sampaio et al. 2008; Holinger et al. 2005; Chiang et al. 2007). Importantly, brain alterations in individuals with WS also involve white matter abnormalities (Hoeft et al. 2007; Marenco et al. 2007). Specifically, corpus callosum (CC), the major white matter fiber bundle responsible for homotopic and heterotopic interhemispheric connections (Paul et al. 2007), has also been studied in this syndrome. Fibers of the CC are implicated in a wide range of cognitive abilities, such as binocular coordination skills (Johansen-Berg et al. 2007), visual attention (Hines et al. 2002), processing speed (Schulte et al. 2005), reading and intelligence (Luders et al. 2007b), and comprehension of syntax and linguistic pragmatics (Paul et al. 2007). Of note, all of these cognitive functions have been found to be affected in WS (Karmiloff-Smith et al. 2003). Previous studies that have analyzed the CC in WS reported morphologic abnormalities and volumetric reductions, particularly in the posterior component of CC (Luders et al. 2007a; Schmitt et al. 2001a, b; Tomaiuolo et al. 2002). Specifically, midsagittal CC area and midline length were found to be reduced in WS, with absolute reductions of whole CC being more pronounced in the posterior part of CC (splenium and isthmus), even when relative volumes were compared (Schmitt et al. 2001a, b). In addition, the CC is reported to be shorter and with a larger bending angle in WS than in typically developing individuals (Luders et al. 2007a; Schmitt et al. 2001b; Tomaiuolo et al. 2002).

Of note, the majority of these studies have used Witelson's geometric classification of callosal regions (Witelson 1989) and only volumetric measurements have been included. However, recent reports, based on tractography analysis, propose new landmarks for defining callosal sections, which provide a better description of CC with respect to the microstructure level of this brain region (Hofer and Frahm 2006), when comparing with geometric-based divisions.

The current study is the first to provide a detailed characterization of CC using a tractography-assisted white matter segmentation approach and a new shape analysis method. We used this multimethod approach because we hypothesized that neurodevelopmental abnormalities might involve both volume change as well as deformation of structure. In addition, taking into account that CC exhibits a continuous growing pattern during adolescence, in parallel to other white matter brain regions (Giedd et al. 1999a, b; McLaughlin et al. 2007), we studied the associations between CC, age and white matter volumes, as well as between cognitive and callosal measures.

We predicted absolute volumetric CC reduction in WS in parallel to atypical morphological patterns, when compared to typically developing individuals. We expected that these differences were more prominent in anterior and posterior CC regions.

Method

Participants

In this study, seventeen participants (7 males), diagnosed with WS (age 19.29 ± 6.29 ; age range 11–34 years; mean Full Scale IQ: 47.87 ± 7.86 ; range 40–62) were compared with 17 typically developing individuals (TD 6 males; age 21.29 ± 7.07 ; age range 11–34 years; mean Full Scale IQ: 109.54 ± 12.00 ; range 90–127). There was no group differences with respect to age ($t(32) = -0.87$, $p > 0.05$), although they differed in mean Full Scale IQ ($t(26^1) = -18.07$, $p < 0.001$). Participants with WS were recruited at the Genetic Medical Institute (Portugal) and the Genomic Foundation in Galicia (Spain). WS diagnoses were made by fluorescent in situ hybridization for confirmation of elastin gene deletion (Ewart et al. 1993). Controls were typically developing individuals with no evidence of psychiatric, neurological disorder or cognitive impairment. Taking into account evidence that CC morphology may be distinctly different in left handed individuals with WS than in left handed TD controls (Martens et al. 2012), all participants from the WS group were right handed, according to the Edinburgh handedness inventory (Oldfield 1971)—some of these participants were also involved in a EEG study (Pinheiro et al. 2010). One participant from the TD group was left handed, but was we decided to include him in the analysis because there is previous evidence showing the absence of significant differences between right and left handers when comparing callosal thickness (Luders et al. 2010, 2011). The Ethical Board approved this study and written informed consent was obtained prior to enrolment from all participating individuals and/or their parents (when individuals were age under 18 years or had a legal representative).

Cognitive assessment

To assess general cognitive functioning, participants were administered the Wechsler Intelligence Scales (Wechsler 1991, 1997).

MRI acquisition and processing

MRI images were obtained on a 1.5-T General Electric system (GE Medical Systems). The scan acquisition protocol

¹ FSIQ was not available for two participants in TD group.

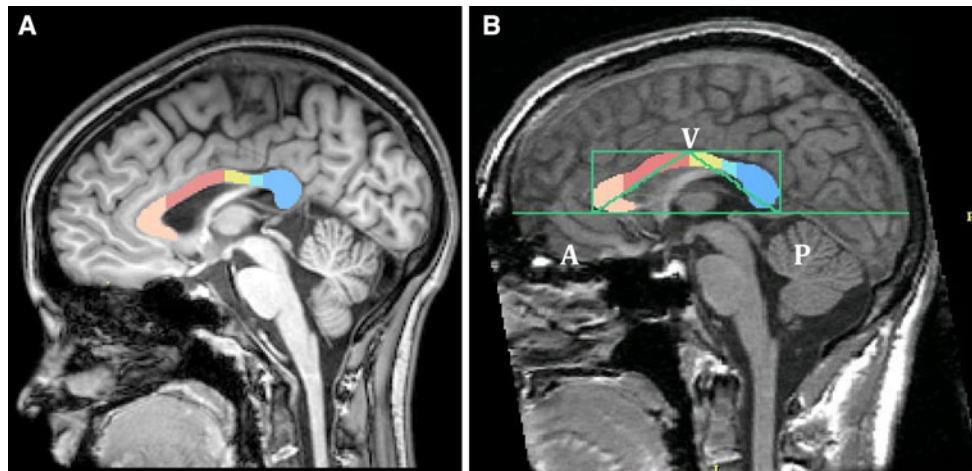


Fig. 1 **a** CC sections segmentation, **b** CC length (A – P) and bending angle: A anterior, P posterior, V vertex

consisted of contiguous 1.5-mm slices of the whole brain. Coronal T1 (SPGR), TE = 5 ms, TR = 35 ms, 256×192 matrix, 1.5 mm thickness and an axial PD/T2 (TE = 30 ms, TR = 3,000 ms) sequence were aligned. Images were aligned using the line between the anterior and posterior commissures and the sagittal sulcus to correct head tilt and were also resampled to make voxels isotropic (sides measured 0.9375 mm). Then, an atlas-based expectation maximization (EM) segmentation program separated raw MR data into cerebrospinal fluid (CSF), gray matter and white matter volumes (Pohl et al. 2007) and total intracranial volume (ICV) was computed as the sum of white matter, gray matter and CSF volumes. The individual volume of CC regions was calculated using the 3D slicer software for segmentation (<http://www.slicer.org/>).

Regions of interest definition

Measurement of the corpus callosum

The sagittal slice that included the clearest view of the corpus callosum, aqueduct, tectum, septum pellucidum, and falx, was chosen as the midsagittal slice. This slice and two slices laterally on each side ($N = 5$ slices) were manually segmented, and volume of the entire corpus and the five CC subsections (number of voxels) was calculated for each of the five slices, using 3D slicer software (Frumin et al. 2002).

Measurement of CC subregions

Although the majority of studies subdivide CC according to Witelson's geometric classification (Witelson 1989), other proposals performing DTI-based CC subdivisions, suggest new landmarks for defining callosal sections (Hofer and Frahm 2006). Thus, for this study, CC was segmented based on a classification method of five vertical CC partitions

(Hofer and Frahm 2006), which provides a better description of CC at the connectivity and microstructural level of this brain region. Specifically, region I connects prefrontal areas; region II contains fibers that connect premotor and supplementary motor areas; region III is composed by fibers that connects to primary motor area; region IV connects primary sensory areas in parietal and temporal lobes; and region V encompasses fibers that connect parietal, temporal, and occipital lobes (Hofer and Frahm 2006). Specifically, i.e. five vertical CC partitions were segmented along the midline between the most frontal (A) to the most posterior (P) points in five slices (see Fig. 1a).

Global shape measures

We extracted two measures to describe the overall shape of the midsagittal section of the CC. First, the midline length was computed in the midsagittal slice as the distance between the most anterior (A) and posterior (P) points of CC. Second, the bending angle was measured as described previously (Tomaiuolo et al. 2002). Briefly, in the midsagittal slice, a horizontal line was drawn at the most inferior level of CC, the most anterior (A) and posterior (P) part of CC on this line was labeled. Then, the bounding box of CC was drawn as a rectangle and a third landmark (V) was placed on the superior line of the rectangle at the midpoint between (A) and (P). The distance [AP] is the midline length, and the angle (AVP) is the so-called bending angle—see Fig. 1b.

Skeletal shape analysis

A two-dimensional skeleton of the CC was extracted in the mid-sagittal slice. Two landmarks were positioned at the anterior and posterior tips of CC and the algorithm of Bouix and Siddiqi (2005) was used to extract the 2D

skeleton by “peeling” layers of the object until only the central line remained. This line was then smoothed and parametrized by arc length by fitting a cubic smoothing spline to the data. The result is a 2D curve composed of 100 equally spaced vertices on the curve (see Fig. 2a). This process makes it possible to compare directly the specific location along a skeleton across individuals as they all have identical parametrization. At each vertex the distance from the skeleton to the boundary of the midsagittal CC (we call this measure thickness), as well as the curvature of the skeletal line are recorded.

Data analysis

All volumetric, bending angle, midline length and volume data met the criteria for using parametric tests, including normality and variance homogeneity. Thus, group differences were analyzed with the Student’s *t* test. Taking into account that groups were matched on chronological age, intracranial volume (ICV) was used as covariate in all computations, with the exception of CC length variable, where we opted to use age and anterior–posterior length of cerebrum in the midsagittal slice (as we considered this to be a better morphological variable to control for this measure). Thus, MANCOVAs were performed, using CC measures as dependent variables, with diagnosis as fixed effects (WS and typically developing subjects), and ICV volume as covariate. A $p < 0.05$ was assumed to denote significant difference. Effect sizes were reported for group comparisons.

For skeletal shape differences, we measured the following quantities at each vertex along the skeletal curve: curvature, distance from the vertex to the boundary (thickness), and thickness normalized by the area of the CC midsagittal section. The mean of each of these values was computed over each population at each vertex and compared using a non-parametric permutation test (Good 2005). Given the large number of vertices on the curve and the small sample size, the resulting p values were corrected for multiple comparisons using the false discovery rate (FDR) at the 5 % level (Nichols 2003).

We analyzed the developmental trajectories of callosal regions, performing a correlational analysis between age, CC and CC subsections volume [ICV was not correlated with age in WS ($r = -0.33$, $p < 0.05$) and TD ($r = -0.35$, $p < 0.05$)]. Correlational analyses between Verbal IQ (VIQ), Performance IQ (PIQ), Full Scale IQ (FSIQ), Factorial Indexes (Processing Speed and Perceptual Organization) and general measures of CC (length and volume) were performed for both groups separately (controlling for age effects). Additionally, we performed a correlational analysis between volumes of the different regions of CC (I, II, III, IV and V sections) and IQ measures—VIQ, PIQ and

FSIQ. The Fisher *r*-to-*z* transformation was used to assess the significance of the difference between two correlation coefficients observed in both groups.

Results

Global shape indices

We found no group differences regarding the bending angle, although a trend towards a larger angle in WS ($M = 112.87 \pm 8.25$) when compared with TD ($M = 108.93 \pm 5.19$) could be observed ($t(32) = 1.67$, $p = 0.11$). However, when ICV volume was used as covariate, a significant group effect emerged ($F(1,32) = 5.59$, $p < 0.05$), with WS showing an increased CC angle. The absolute midline CC length was also significantly reduced in WS ($t(32) = -3.04$, $p < 0.01$) and when anterior–posterior distance of cerebrum in the midsagittal line was computed as covariate ($F(1,32) = 4.83$, $p < 0.05$).

CC volume indices

Analyses of CC volumes showed a statistically significant reduction in WS for the entire CC [WS, $M = 2.40 \pm 0.33$; TD = 2.83 ± 0.45 ; $t(32) = -3.14$, $p < 0.01$], and in all CC subdivisions [section I, $M_{WS} = 0.68 \pm 0.09$; $M_{TD} = 0.77 \pm 0.12$; $t(32)_I = -2.38$, $p < 0.05$; section III, $M_{WS} = 0.23 \pm 0.06$; $M_{TD} = 0.29 \pm 0.05$, $t(32)_{III} = -2.78$, $p < 0.01$; section IV, $M_{WS} = 0.10 \pm 0.03$; $M_{TD} = 0.13 \pm 0.03$, $t(32)_{IV} = -2.71$, $p < 0.05$; section V, $M_{WS} = 0.71 \pm 0.09$, $M_{TD} = 0.88 \pm 0.13$; $t(32)_V = -4.07$, $p < 0.001$], except for section II ($M_{WS} = 0.67 \pm 0.13$; $M_{TD} = 0.76 \pm 0.15$; $t(32)_{II} = -1.93$, $p = 0.06$). Using MANCOVA to control for the effects of ICV, the group differences remained for total mean CC volume ($F(1,32) = 5.97$, $p < 0.05$) and for the different callosal subsections [$F(1,32)_{II} = 4.94$, $p < 0.05$; $F(1,32)_{III} = 5.06$, $p < 0.05$; $F(1,32)_{IV} = 6.14$, $p < 0.05$; $F(1,32)_V = 5.21$, $p < 0.05$]. No group differences were observed regarding section I [$F(1,32)_I = 2.97$, $p = 0.09$].

Skeletal line indices

To further evaluate the shape of CC, we analyzed the curvature and thickness along its skeletal curve (Fig. 2b). As thickness is highly correlated with the area of the CC midsagittal section, we also analyzed the thickness normalized by this area. Our results showed significant group differences with respect to skeletal curvature, that is, CC in the WS group was more curved in the posterior part (Fig. 2b). No significant difference in absolute thickness profile (Fig. 2b) was found, but normalized thickness was

Fig. 2 **a** Top CC and extracted skeleton. *Bottom* the corresponding smoothed and arc length parametrized skeleton. This example is parametrized with 50 equally spaced vertices (*blue dots*) for display purposes, although in our experiments, we use 100 vertices for better spatial resolution. **b** Statistical analysis along the CC skeleton. On the *left side*, the *x* axis represents the index of 100 vertices equally spaced along the skeleton. The *y* axis is the dependent measure at the corresponding vertex location (*top* curvature, *middle* local thickness, *bottom* local thickness normalized by CC midsagittal area). *Solid lines* represent mean values for each population and *dashed lines* ± 1 standard deviation. On the *right side*, the mean skeleton for the entire population is displayed with *black circles* at vertices where the dependent measure leads to a raw $p < 0.05$, and the *red circles* for vertices where the dependent measure leads to a p value surviving the multiple comparison correction using FDR. The posterior part of the CC (splenium) shows curvature differences. Unnormalized thickness never survives the multiple correction procedure. Normalized thickness reaches significance over the entire length of the CC skeleton

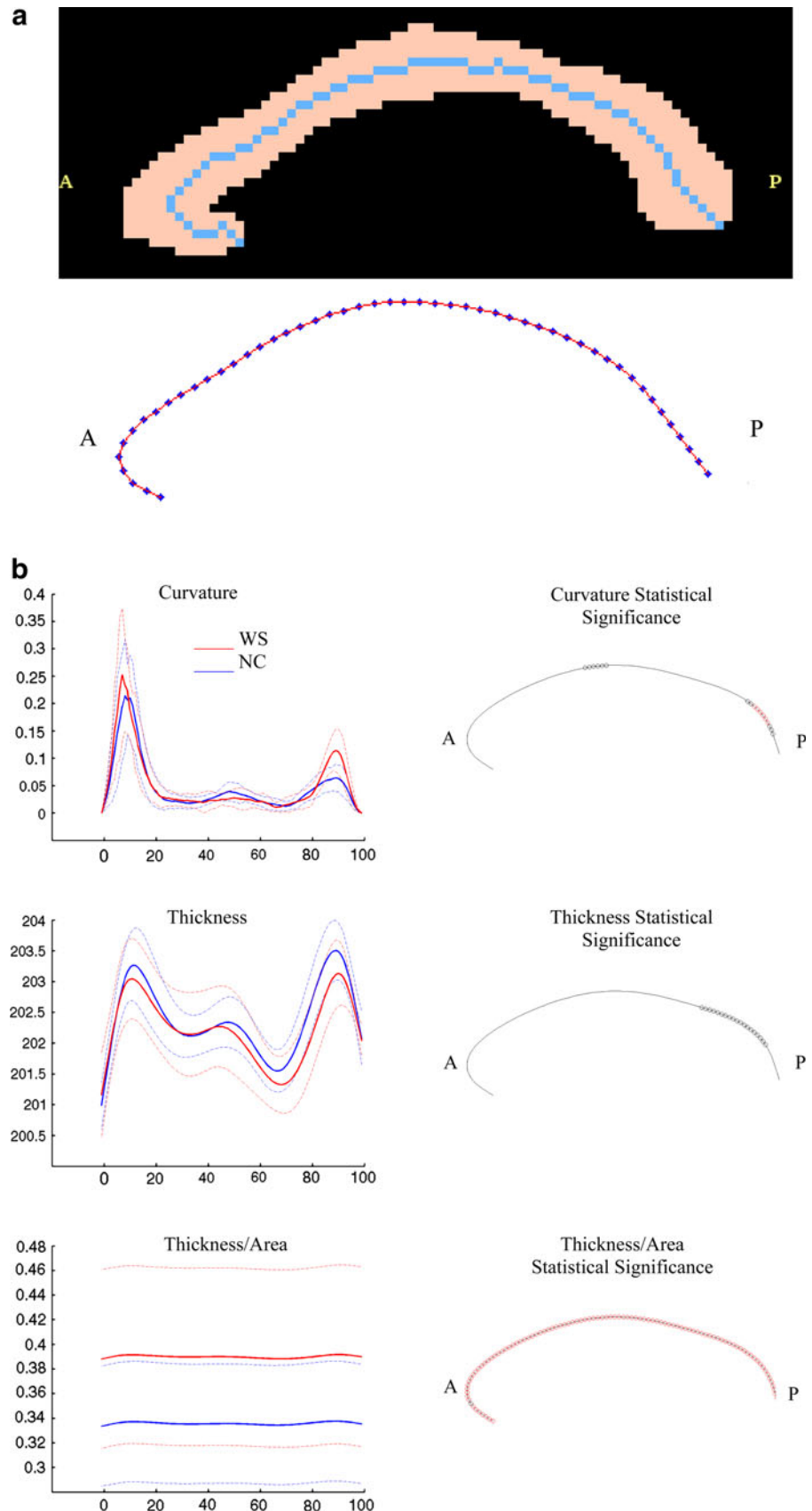


Table 1 Correlations between age, white matter volume and callosal sections

| | CC | Section I | Section II | Section III | Section IV | Section V |
|----------------------------|---------------|---------------|---------------|--------------|-----------------|-----------------|
| Age | | | | | | |
| WS | $r = 0.34$ | $r = 0.06$ | $r = 0.35$ | $r = 0.39$ | $r = 0.48$ | $r = 0.26$ |
| TD | $r = 0.49^*$ | $r = 0.31$ | $r = 0.57^*$ | $r = 0.54^*$ | $r = 0.63^{**}$ | $r = 0.35$ |
| Fisher's Z test | $Z = -0.48$ | $Z = -0.69$ | $Z = -0.75$ | $Z = -0.51$ | $Z = -0.58$ | $Z = -0.26$ |
| White matter volume | | | | | | |
| WS | $r = -0.14$ | $r = -0.19$ | $r = -0.22$ | $r = -0.03$ | $r = -0.11$ | $r = 0.06$ |
| TD | $r = 0.56^*$ | $r = 0.49$ | $r = 0.41$ | $r = 0.51$ | $r = 0.42$ | $r = 0.65^{**}$ |
| Fisher's Z test | $Z = -2.05^*$ | $Z = -1.93^*$ | $Z = -1.74^*$ | $Z = -1.57$ | $Z = -1.48$ | $Z = -1.89^*$ |

* $p < 0.05$, ** $p < 0.01$

found to be significantly different between groups along the entire skeletal curve (Fig. 2b). These results were similar when we normalized thickness to cerebral tissue volumes (to both white matter and ICV volumes). More specifically, we observed a larger relative thickness of CC in WS, when compared with controls.

Developmental trajectories

Developmental trajectories of callosal regions were analyzed, correlating age with CC and regional sections volume. In the typically developing group, age was positively correlated with the volume of the callosal subregions (with the exception of sections I and V), however, no pattern of correlations between age and callosal measures were found in WS. Also, in the typically developing group, CC volume and section V subregion were positively correlated with white matter volume, whereas no correlation was again found in the WS group. Most interestingly, the difference between these correlations (WS vs. TD) was significant for CC, sections I, II and V (see Table 1).

Correlation with cognitive functioning

Partial correlations between general callosal measures (CC volume and midline length) and cognitive performance (FSIQ, VIQ, PIQ and Processing Speed Index) were performed, controlling for the effect of age (see Table 2). Additional correlational analysis were performed between volumes of the different regions of CC (I, II, III, IV and V sections) and IQ measures—see Table 3. Specifically, the results showed that in the typically developing group, the speed of processing index was correlated with CC volume ($r = 0.88$, $p < 0.01$) and with CC length ($r = 0.67$, $p < 0.05$). In addition, VIQ was also correlated with CC length ($r = 0.81$, $p < 0.01$) and with section IV ($r = 0.60$, $p < 0.05$). Again, in this group, a trend was also observed for the association between FSIQ and Length of CC ($r = 0.59$, $p = 0.07$). No correlations were observed in the

WS group and the differences between these correlations (WS vs. TD) were significant for speed of processing index and CC volume and length, FSIQ, VIQ and CC length; as well as for VIQ and sections IV and V.

Discussion

This study is the first to use a multimethod approach to the study of CC, namely a combination of morphometric and shape measures to provide a comprehensive characterization of the CC in WS and relationship with cognitive abilities.

Absolute volumetric reductions of CC (mean CC and subsections) were observed in WS, when compared to typically developing individuals. These results remained after controlling for ICV in all CC measures but region I, and are consistent with previous evidence showing CC absolute and relative volumetric reductions, albeit more prominent in posterior regions (Luders et al. 2007a; Schmitt et al. 2001a, b; Tomaiuolo et al. 2002). The relative preservation of region I (CC region that connects prefrontal areas) is consistent with both neuroanatomical and behavioural data in WS (Capitao et al. 2011a; Chiang et al. 2007). Specifically, a relative preservation of prefrontal, orbitofrontal and anterior cingulate volumes (Chiang et al. 2007) associated with a distinctive social/affective/emotional profile has been illustrated in WS (Porter et al. 2007; Mobbs et al. 2007; Capitao et al. 2011a).

Regional heterogeneity of CC growth is known to occur during development; whereas between 6 and 15 years there is a consistent growth of CC sections connecting temporoparietal regions, between 7 and 11 years, a rapid focal growth at the callosal isthmus contrasts with the stability of splenium and rostrum (Thompson et al. 2000). This suggests that sharp local increases may not be apparent with conventional volumetric methods but can be pursued with a more detailed shape analysis method. The combination of volumetric data with shape analysis provides a more

Table 2 Correlations between overall CC and cognitive measures

| | FSIQ | VIQ | PIQ | Speed of processing index |
|-----------------|-------------------|-------------------|-------------|---------------------------|
| CC volume | | | | |
| WS | $r = -0.21$ | $r = -0.03$ | $r = -0.47$ | $r = -0.06$ |
| TD | $r = -0.13$ | $r = -0.44$ | $r = 0.16$ | $r = 0.88^{**}$ |
| Fisher's Z test | $Z = -0.21$ | $Z = -1.12$ | $Z = -0.89$ | $Z = -3.34^{***}$ |
| CC length | | | | |
| WS | $r = -0.27$ | $r = -0.20$ | $r = -0.24$ | $r = -0.09$ |
| TD | $r = 0.59$ | $r = 0.81^{**}$ | $r = 0.19$ | $r = 0.67^*$ |
| Fisher's Z test | $Z = -2.43^{***}$ | $Z = -3.38^{***}$ | $Z = -1.11$ | $Z = -2.29^*$ |

* $p < 0.05$, ** $p < 0.01$, *** $p < 0.001$

Table 3 Correlations between CC regions and cognitive measures

| | FSIQ | VIQ | PIQ |
|-----------------|-------------|---------------|-------------|
| CC section I | | | |
| WS | $r = 0.28$ | $r = 0.19$ | $r = 0.34$ |
| TD | $r = 0.23$ | $r = 0.36$ | $r = -0.12$ |
| Fisher's Z test | $Z = 0.11$ | $Z = -0.37$ | $Z = 0.96$ |
| CC section II | | | |
| WS | $r = 0.25$ | $r = 0.22$ | $r = 0.38$ |
| TD | $r = 0.11$ | $r = 0.34$ | $r = -0.14$ |
| Fisher's Z test | $Z = 0.29$ | $Z = -0.26$ | $Z = 1.1$ |
| CC section III | | | |
| WS | $r = 0.14$ | $r = 0.05$ | $r = 0.37$ |
| TD | $r = 0.11$ | $r = 0.32$ | $r = -0.23$ |
| Fisher's Z test | $Z = 0.06$ | $Z = -0.57$ | $Z = 1.26$ |
| CC section IV | | | |
| WS | $r = -0.22$ | $r = -0.16$ | $r = 0.03$ |
| TD | $r = 0.44$ | $r = 0.60^*$ | $r = 0.13$ |
| Fisher's Z test | $Z = -1.41$ | $Z = -1.73^*$ | $Z = -0.02$ |
| CC section V | | | |
| WS | $r = -0.15$ | $r = -0.17$ | $r = 0.09$ |
| TD | $r = 0.44$ | $r = 0.55$ | $r = 0.36$ |
| Fisher's Z test | $Z = -1.26$ | $Z = -1.70^*$ | $Z = -0.06$ |

* $p < 0.05$

powerful tool to detect subtle differences in CC white matter. Therefore, we added a shape analysis of CC, which included several parameters, namely the bending angle, CC length, thickness and curvature. We observed a trend for a larger bending angle and lower curvature in the middle of the CC skeleton in WS when compared with typically developing individuals. This indicates an overall “flatter” less convex CC, which is in agreement with previous reports (Luders et al. 2007a; Schmitt et al. 2001a, b; Tomaiuolo et al. 2002). In addition, we found a higher curvature in the posterior part of the CC skeleton, indicating a slightly more convex shape in this area, a result not reported elsewhere. Interestingly, a less curved CC was accompanied by a more curved and premature posterior CC

ending, suggesting abnormal cortico-cortical connections between the parietal and occipital lobes in WS (Meyer-Lindenberg et al. 2004). Indeed, smaller volumes of the parietal and occipital lobes (Eckert et al. 2005; Reiss et al. 2004) together with abnormal gyrification patterns (Gaser et al. 2006; Thompson et al. 2005) and increased cell packing density (Galaburda et al. 2002) in these regions have been associated with one of the most remarkable features of the WS cognitive profile—their profound deficit in performing visuo-spatial and constructive tasks. In addition, and despite volumetric reductions, a relative increase of CC thickness was observable in WS, which expands previous evidence of small local increases in CC thickness in WS (Luders et al. 2007a).

In agreement with altered CC structure and morphology in WS, a different allometric relationship with age, white matter volume and callosal measures were observed in both groups. Specifically, the absence of an allometric growth between individual subregions of the CC with either white matter volume or age in WS is also a finding in other developmental disorders (Cascio et al. 2006), suggesting a disconnection between CC and white matter. Indeed, a distinct pattern was observed in the typically developing group, where the area of CC was positively correlated with age and total white matter volume. This result confirms the findings of extended growth of CC with age (Giedd et al. 1999a, b; McLaughlin et al. 2007) with white matter volume following the same pattern. Linear increases in white matter with age have been widely reported in typical development (Barnea-Goraly et al. 2005; Giedd et al. 1999a, b; Keshavan et al. 2002; Reiss et al. 1996), indicating that brain circuits become more coherent and myelinated, particularly in areas involved with complex cognitive functions (Barnea-Goraly et al. 2005).

Finally, callosal measures were positively associated with improved performances in FSIQ, speed of processing and visual attention only in the typically developing group, a result that is in accordance with previous reports (Schulte et al. 2005; Hines et al. 2002), but not observed in our clinical group. Although these results do not allow us to clearly state that CC abnormalities in WS may be associated with cognitive deficits, we have obtained indirect evidence that partially support this hypothesis. First, we observed reduced volumetry and abnormal shape in caudal areas of the CC, brain regions associated with visuo-spatial functioning (Eckert et al. 2005; Meyer-Lindenberg et al. 2004), an important hallmark of WS cognitive architecture. Second, both groups diverge regarding the correlation patterns between callosal measures and IQ, suggesting that this may reflect less inter-hemispheric transfer, affecting visual and verbal information processing in WS. Finally, CC data in a variety of other developmental disorders (e.g. autism, schizophrenia, Tourette's syndrome and developmental delay disorder) reinforces this hypothesis, namely showing an association between callosal measures (shape and size) and certain behavioural, social, language and attention features. For example, an association between callosal thinning (Vidal et al. 2006; Hardan et al. 2009) and clinical features of autism, such as social deficits, repetitive behaviors and sensory abnormalities, have been reported (Hardan et al. 2009). In a different direction, increased CC size and thickness were positively with psychopathic antisocial personality (Raine et al. 2003) and with severity of tics in Tourette's syndrome (Plessen et al. 2004).

The results from this study show evidence of abnormal CC volume, shape and thickness profiles in WS. Together,

this integrated approach is consistent with the fact that morphogenesis changes of the CC are associated with complex mechanical and genetic factors (Van Essen 1997). Interestingly, midline structures are the most vulnerable to the effects of physical and mechanical properties of morphogenetic mechanisms that model shape during brain development (Van Essen 1997; Van Essen and Drury 1997; Van Essen et al. 1998), including the corpus callosum (Lenroot and Giedd 2006). Indeed, previous evidence reporting midline brain regions abnormalities in WS must be considered (Meyer-Lindenberg et al. 2005; Capitao et al. 2011b; Sampaio et al. 2010). Furthermore, WS is a genetic disorder in which several genes are implicated, including FZD3 and FZD9, that are part of *Wnt* signalling pathways involved in convergence and extension control mechanisms (e.g. axon elongation) in mammals (Lindwall et al. 2007). This evidence suggests that deletion of genes within WSCR may play an important role in the mechanisms that model shape and regulate timing of CC axonal growth/migration/pruning in specific developmental growth windows. Specifically, a shorter, curvier, thicker but overall smaller CC in WS may reflect more neuronal aggregation due to greater cell packing densities and/or decreased fiber pruning during development. Indeed, research has shown that callosal axons are eliminated postnatally throughout adulthood (Raine et al. 2003; LaMantia and Rakic 1990) and that extensive postnatal axonal growth of CC (Thompson et al. 2000; Giedd et al. 1999a) is likely due to an increased myelination of the CC fibers. This CC axon elimination and myelination can be related to increased synaptic density throughout the cerebral cortex (LaMantia and Rakic 1990; Hardan et al. 2009). and reflect increased inter-hemispheric transfer. Therefore, a possible decreased inter-hemispheric transfer may be associated with cognitive functioning in WS, which is in accordance with other studies showing increased callosal size and abnormal interhemispheric transfer (e.g. Raine et al. 2003).

A limitation of the current study concerns the size of the samples and the fact that all individuals with WS displayed moderate intellectual disabilities. Larger samples will be needed in future studies to allow the generalization of these findings and incorporate new white matter assessment tools like diffusion tensor imaging.

In summary, CC morphometry and shape were evaluated in WS and typically developing individuals. We found group differences regarding absolute and relative volumes and CC shape, suggesting that CC abnormalities may contribute to neurocognitive difficulties in WS, in particular social-emotional and visuo-spatial functioning. Abnormal shape morphology of the CC could help to clarify structural deformities associated with abnormal neurodevelopment processes.

Acknowledgments This research was supported by the grants PIC/IC/83290/2007 and PTDC/PSI-PCL/115316/2009 from Fundação para a Ciência e Tecnologia (Portugal). This study was also supported, in part, by grants from the National Institutes of Health (K05 MH070047).

Conflict of interest The authors report no conflicts of interest.

References

- Barnea-Goraly N, Menon V, Eckert M, Tamm L, Bammer R, Karchemskiy A, Dant CC, Reiss AL (2005) White matter development during childhood and adolescence: a cross-sectional diffusion tensor imaging study. *Cereb Cortex* 15(12):1848–1854
- Bellugi U, Adolphs R, Cassady C, Chiles M (1999) Towards the neural basis for hypersociability in a genetic syndrome. *NeuroReport* 10(8):1653
- Bellugi U, Lichtenberger L, Jones W, Lai Z, St George M (2000) The neurocognitive profile of Williams Syndrome: a complex pattern of strengths and weaknesses. *J Cogn Neurosci* 12(Suppl 1):7–29
- Bouix S, Siddiqi K (2005) Optics, mechanics and Hamilton–Jacobi skeletons. *Adv Imaging Electron Phys* 135:1–39
- Capitao L, Sampaio A, Fernandez M, Sousa N, Pinheiro A, Goncalves OF (2011a) Williams syndrome hypersociability: a neuropsychological study of the amygdala and prefrontal cortex hypotheses. *Res Dev Disabilities* 32(3):1169–1179
- Capitao L, Sampaio A, Sampaio C, Vasconcelos C, Fernandez M, Garayzabal E, Shenton ME, Goncalves OF (2011b) MRI amygdala volume in Williams syndrome. *Res Dev Disabilities* 32(6):2767–2772
- Cascio C, Styner M, Smith RG, Poe MD, Gerig G, Hazlett HC, Jomier M, Bammer R, Piven J (2006) Reduced relationship to cortical white matter volume revealed by tractography-based segmentation of the corpus callosum in young children with developmental delay. *Am J Psychiatry* 163(12):2157–2163
- Chiang MC, Reiss AL, Lee AD, Bellugi U, Galaburda AM, Korenberg JR, Mills DL, Toga AW, Thompson PM (2007) 3D pattern of brain abnormalities in Williams syndrome visualized using tensor-based morphometry. *Neuroimage* 36(4):1096–1109
- Eckert MA, Hu D, Eliez S, Bellugi U, Galaburda A, Korenberg J, Mills D, Reiss AL (2005) Evidence for superior parietal impairment in Williams syndrome. *Neurology* 64(1):152–153
- Ewart A, Morris C, Atkinson D, Jin W, Sternes K, Spallone P, Stock AD, Leppert M, Keating M (1993) Hemizygoty at the elastin locus in a developmental disorder. Williams syndrome. *Nat Genet* 5(1):11–16
- Frumin M, Golland P, Kikinis R, Hirayasu Y, Salisbury DF, Hennen J, Dickey CC, Anderson M, Jolesz FA, Grimson WE, McCarter RW, Shenton ME (2002) Shape differences in the corpus callosum in first-episode schizophrenia and first-episode psychotic affective disorder. *Am J Psychiatry* 159(5):866–868
- Galaburda AM, Holinger DP, Bellugi U, Sherman GF (2002) Williams syndrome: neuronal size and neuronal-packing density in primary visual cortex. *Arch Neurol* 59(9):1461–1467
- Gaser C, Luders E, Thompson PM, Lee AD, Dutton RA, Geaga JA, Hayashi KM, Bellugi U, Galaburda AM, Korenberg JR, Mills DL, Toga AW, Reiss AL (2006) Increased local gyrification mapped in Williams syndrome. *Neuroimage* 33(1):46–54
- Giedd JN, Blumenthal J, Jeffries N, Rajapakse JC, Vaituzis AC, Liu H, Berry YC, Tobin M, Nelson J, Castellanos FX (1999a) Development of the human corpus callosum during childhood and adolescence: a longitudinal MRI study. *Prog Neuro-Psychopharmacol Biol Psychiatry* 23:571–588
- Giedd JN, Blumenthal J, Jeffries NO, Castellanos FX, Liu H, Zijdenbos A, Paus T, Evans AC, Rapoport J (1999b) Brain development during childhood and adolescence: a longitudinal MRI study. *Nat Neurosci* 2:861–863
- Good P (2005) Permutation, parametric, and bootstrap tests of hypotheses, 3rd edn. New York
- Hardan AY, Pabalan M, Gupta N, Bansal R, Melhem NM, Fedorov S, Keshavan MS, Minshew NJ (2009) Corpus callosum volume in children with autism. *Psychiatry Res* 174(1):57–61
- Hines RJ, Paul LK, Brown WS (2002) Spatial attention in agenesis of the corpus callosum: shifting attention between visual fields. *Neuropsychologia* 40(11):1804–1814
- Hoefl F, Barnea-Goraly N, Haas BW, Golarai G, Ng D, Mills D, Korenberg J, Bellugi U, Galaburda A, Reiss AL (2007) More is not always better: increased fractional anisotropy of superior longitudinal fasciculus associated with poor visuospatial abilities in Williams syndrome. *J Neurosci* 27(44):11960–11965
- Hofer S, Frahm J (2006) Topography of the human corpus callosum revisited-comprehensive fiber tractography using diffusion tensor magnetic resonance imaging. *Neuroimage* 32(3):989–994
- Holinger DP, Bellugi U, Mills DL, Korenberg JR, Reiss AL, Sherman GF, Galaburda AM (2005) Relative sparing of primary auditory cortex in Williams Syndrome. *Brain Res* 1037(1–2):35–42
- Johansen-Berg H, Della-Maggiore V, Behrens TE, Smith SM, Paus T (2007) Integrity of white matter in the corpus callosum correlates with bimanual co-ordination skills. *Neuroimage* 36(Suppl 2):T16–T21
- Karmiloff-Smith A, Brown JH, Grice S, Paterson S (2003) Dethroning the myth: cognitive dissociations and innate modularity in Williams syndrome. *Dev Neuropsychol* 23(1–2):227–242
- Keshavan MS, Diwadkar VA, DeBellis M, Dick E, Kotwal R, Rosenberg DR, Sweeney JA, Minshew N, Pettegrew JW (2002) Development of the corpus callosum in childhood, adolescence and early adulthood. *Life Sci* 70(16):1909–1922
- Klein-Tasman B, Mervis C (2003) Distinctive personality characteristics of 8-, 9-, and 10-year-olds with Williams syndrome. *Dev Neuropsychol* 23(1):269–290
- LaMantia AS, Rakic P (1990) Axon overproduction and elimination in the corpus callosum of the developing rhesus monkey. *J Neurosci* 10(7):2156–2175
- Lenroot RK, Giedd JN (2006) Brain development in children and adolescents: insights from anatomical magnetic resonance imaging. *Neurosci Biobehav Rev* 30:718–729
- Lindwall C, Fothergill T, Richards LJ (2007) Commissure formation in the mammalian forebrain. *Curr Opin Neurobiol* 17(1):3–14
- Luders E, Di Paola M, Tomaiuolo F, Thompson PM, Toga AW, Vicari S, Petrides M, Caltagirone C (2007a) Callosal morphology in Williams syndrome: a new evaluation of shape and thickness. *NeuroReport* 18(3):203–207
- Luders E, Narr KL, Bilder RM, Thompson PM, Szeszko PR, Hamilton L, Toga AW (2007b) Positive correlations between corpus callosum thickness and intelligence. *Neuroimage* 37(4):1457–1464
- Luders E, Cherbuin N, Thompson PM, Gutman B, Anstey KJ, Sachdev P, Toga AW (2010) When more is less: associations between corpus callosum size and handedness lateralization. *Neuroimage* 52(1):43–49
- Luders E, Thompson PM, Narr KL, Zamanyan A, Chou YY, Gutman B, Dinov ID, Toga AW (2011) The link between callosal thickness and intelligence in healthy children and adolescents. *Neuroimage* 54(3):1823–1830
- Marengo S, Siuta MA, Kippenhan JS, Grodofsky S, Chang WL, Kohn P, Mervin CB, Morris CA, Weinberger DR, Meyer-Lindenberg A, Pierpaoli C, Berman KF (2007) Genetic contributions to white matter architecture revealed by diffusion tensor imaging in Williams syndrome. *Proc Natl Acad Sci USA* 104(38):15117–15122

- Martens MA, Wilson SJ, Chen J, Wood A, Reutens D (2012) Handedness and corpus callosum morphology in Williams syndrome. *Dev Psychopathol* (in press)
- McLaughlin NC, Paul RH, Grieve SM, Williams LM, Laidlaw D, DiCarlo M, Clark CR, Whelihan W, Cohen RA, Whitford TJ, Gordon E (2007) Diffusion tensor imaging of the corpus callosum: a cross-sectional study across the lifespan. *Int J Dev Neurosci* 25(4):215–221
- Meyer-Lindenberg A, Kohn P, Mervis CB, Kippenhan JS, Olsen RK, Morris CA, Berman KF (2004) Neural basis of genetically determined visuospatial construction deficit in Williams syndrome. *Neuron* 43(5):623–631
- Meyer-Lindenberg A, Mervis CB, Sarpal D, Koch P, Steele S, Kohn P, Marengo S, Morris CA, Das S, Kippenhan S, Mattay VS, Weinberger DR, Berman KF (2005) Functional, structural, and metabolic abnormalities of the hippocampal formation in Williams syndrome. *J Clin Invest* 115(7):1888–1895
- Mobbs D, Eckert MA, Mills D, Korenberg J, Bellugi U, Galaburda AM, Reiss AL (2007) Frontostriatal dysfunction during response inhibition in Williams syndrome. *Biol Psychiatry* 62(3):256–261
- Nichols H (2003) Controlling the familywise error rate in functional neuroimaging: a comparative review. *Stat Methods Med Res* 12(5):419–446
- Oldfield RC (1971) The assessment and analysis of handedness: the Edinburgh inventory. *Neuropsychologia* 9(1):97–113
- Paul LK, Brown WS, Adolphs R, Tyszka JM, Richards LJ, Mukherjee P, Sherr EH (2007) Agenesis of the corpus callosum: genetic, developmental and functional aspects of connectivity. *Nat Rev Neurosci* 8(4):287–299
- Pinheiro AP, Galdo-Alvarez S, Sampaio A, Niznikiewicz M, Gonçalves OF (2010) Electrophysiological correlates of semantic processing in Williams syndrome. *Res Dev Disabil* 31(6):1412–1425
- Plessen KJ, Wentzel-Larsen T, Hugdahl K, Feineigle P, Klein J, Staib LH, Leckman JF, Bansal R, Peterson BS (2004) Altered interhemispheric connectivity in individuals with Tourette's disorder. *Am J Psychiatry* 161(11):2028–2037
- Pohl K, Bouix S, Nakamura M, Rohlfing T, McCarley R, Kikinis R, Grimson W, Shenton ME, Wells W (2007) A hierarchical algorithm for MR brain image parcellation. *IEEE Trans Med Imaging* 26(9):1201–1212
- Porter MA, Coltheart M, Langdon R (2007) The neuropsychological basis of hypersociability in Williams and Down syndrome. *Neuropsychologia* 45(12):2839–2849
- Raine A, Lencz T, Taylor K, Hellige JB, Bihrlle S, Lacasse L, Lee M, Ishikawa S, Colletti P (2003) Corpus callosum abnormalities in psychopathic antisocial individuals. *Arch Gen Psychiatry* 60(11):1134–1142
- Reiss AL, Abrams MT, Singer HS, Ross JL, Denckla MB (1996) Brain development, gender and IQ in children. A volumetric imaging study. *Brain* 119(Pt 5):1763–1774
- Reiss AL, Eckert MA, Rose FE, Karchemskiy A, Kesler S, Chang M, Reynolds MF, Kwon H, Galaburda A (2004) An experiment of nature: brain anatomy parallels cognition and behavior in Williams syndrome. *J Neurosci* 24(21):5009–5015
- Sampaio A, Sousa N, Fernandez M, Vasconcelos C, Shenton ME, Gonçalves OF (2008) MRI assessment of superior temporal gyrus in Williams syndrome. Cognitive and behavioral neurology. *J Soc Behav Cogn Neurol* 21(3):150–156
- Sampaio A, Sousa N, Fernandez M, Vasconcelos C, Shenton ME, Gonçalves OF (2010) Williams syndrome and memory: a neuroanatomic and cognitive approach. *J Autism Dev Disord* 40(7):870–877
- Schmitt JE, Eliez S, Bellugi U, Reiss AL (2001a) Analysis of cerebral shape in Williams syndrome. *Arch Neurol* 58(2):283–287
- Schmitt JE, Eliez S, Warsofsky IS, Bellugi U, Reiss AL (2001b) Corpus callosum morphology of Williams syndrome: relation to genetics and behavior. *Dev Med Child Neurol* 43(3):155–159
- Schulte T, Sullivan EV, Muller-Oehring EM, Adalsteinsson E, Pfefferbaum A (2005) Corpus callosal microstructural integrity influences interhemispheric processing: a diffusion tensor imaging study. *Cereb Cortex* 15(9):1384–1392
- Strømme P, Bjømstad P, Ramstad K (2002) Prevalence estimation of Williams syndrome. *J Child Neurol* 17(4):269
- Thompson PM, Giedd JN, Woods RP, MacDonald D, Evans AC, Toga AW (2000) Growth patterns in the developing brain detected by using continuum mechanical tensor maps. *Nature* 404(6774):190–193
- Thompson PM, Lee AD, Dutton RA, Geaga JA, Hayashi KM, Eckert MA, Bellugi U, Galaburda AM, Korenberg JR, Mills DL, Toga AW, Reiss AL (2005) Abnormal cortical complexity and thickness profiles mapped in Williams syndrome. *J Neurosci* 25(16):4146–4158
- Tomaiuolo F, Di Paola M, Caravale B, Vicari S, Petrides M, Caltagirone C (2002) Morphology and morphometry of the corpus callosum in Williams syndrome: a T1-weighted MRI study. *NeuroReport* 13(17):2281–2284
- Van Essen DC (1997) A tension-based theory of morphogenesis and compact wiring in the central nervous system. *Nature* 385:313–318
- Van Essen DC, Drury HA (1997) Structural and functional analyses of human cerebral cortex using a surface-based atlas. *J Neurosci* 17(18):7079–7102
- Van Essen DC, Drury HA, Joshi S, Miller MI (1998) Functional and structural mapping of human cerebral cortex: solutions are in the surfaces. *Proc Natl Acad Sci USA* 95(3):788–795
- Vidal CN, Nicolson R, DeVito TJ, Hayashi KM, Geaga JA, Drost DJ, Williamson PC, Rajakumar N, Sui Y, Dutton RA, Toga AW, Thompson PM (2006) Mapping corpus callosum deficits in autism: an index of aberrant cortical connectivity. *Biol Psychiatry* 60(3):218–225
- Wechsler D (1991) Wechsler Intelligence Scale for Children. Manual, 3rd edn. Psychological Corporation, San Antonio
- Wechsler D (1997) Wechsler Adult Intelligence Scale. Manual, 3rd edn. Psychological Corporation, San Antonio
- Witelson SF (1989) Hand and sex differences in the isthmus and genu of the human corpus callosum. A postmortem morphological study. *Brain* 112(Pt 3):799–835